

1 **Eco-evolutionary Modelling of Global Vegetation Dynamics and the Impact of CO₂**
2 **during the late Quaternary: Insights from Contrasting Periods**

3 Jierong Zhao¹, Boya Zhou², Sandy P. Harrison^{1,*}, Iain Colin Prentice²

4 ¹ Department of Geography and Environmental Science, University of Reading, Whiteknights,
5 Reading, RG6 6AB, UK

6 ² Georgina Mace Centre for the Living Planet, Department of Life Sciences, Imperial College
7 London, Silwood Park Campus, Buckhurst Road, Ascot, SL5 7PY, UK

8 * Corresponding author: s.p.harrison@reading.ac.uk

9 *Ms for: Earth System Dynamics*

10 **Abstract**

11 Changes in climate have had major impacts on global vegetation during the Quaternary.
12 However, variations in CO₂ levels also play a role in shaping vegetation dynamics by
13 influencing plant productivity and water-use efficiency, and consequently the relative
14 competitive success of the C₃ and C₄ photosynthetic pathways. We use an eco-evolutionary
15 optimality (EEO) based modelling approach to examine the impacts of climate fluctuations and
16 CO₂-induced alterations on gross primary production (GPP). We considered two contrasting
17 periods, the Last Glacial Maximum (LGM, 21,000 years before present) and the mid-Holocene
18 (MH, 6,000 years before present) and compared both to pre-industrial conditions (PI). The
19 LGM, characterised by generally colder and drier climate, had a CO₂ level close to the
20 minimum for effective C₃ plant operation. In contrast, the MH had warmer summers and
21 increased monsoonal rainfall in the northern hemisphere, although with a CO₂ level still below
22 PI. We simulated vegetation primary production at the LGM and the MH compared to the PI
23 baseline using a light-use efficiency model that simulates GPP coupled to an EEO model that
24 simulates leaf area index (LAI) and C₃/C₄ competition. We found that low CO₂ at the LGM
25 was nearly as important as climate in reducing tree cover, increasing the abundance of C₄ plants
26 and lowering GPP. Global GPP in the MH was similar to the PI (although greater than the
27 LGM), also reflecting CO₂ constraints on plant growth despite the positive impacts of warmer
28 and/or wetter climates experienced in the northern hemisphere and tropical regions. These
29 results emphasise the importance of taking account of impacts of changing CO₂ levels on plant
30 growth to model ecosystem changes.

31 1 Introduction

32 Vegetation regulates the exchanges of energy, water, and carbon dioxide between the land and
33 the atmosphere (Williams and Torn, 2015; Forzieri et al., 2020; Hoek van Dijke et al., 2020).
34 Gross primary production (GPP), defined as the carbon uptake by vegetation through
35 photosynthesis at the ecosystem scale, determines the extent to which the terrestrial biosphere
36 can mitigate CO₂ emissions (Bonan, 2008; Zeng et al., 2017; Chen et al., 2019). There is a tight
37 coupling between CO₂ uptake and water loss via stomata, such that when ambient CO₂ is high
38 water-use efficiency (the amount of water required for transpiration to achieve a unit of CO₂
39 assimilation) is also high (Medlyn et al., 2017). Recent global greening trends are thought to
40 reflect both changes in climate, particularly warming at high latitudes, and the effect of
41 increasing CO₂ on water-use efficiency (Cai and Prentice, 2020; Piao et al., 2020). However,
42 there is still uncertainty about the relative importance of these two effects on recent changes in
43 global GPP, in part because recent climate changes have been largely driven by the increase in
44 CO₂.

45 Past climate states provide opportunities to examine the role of climate and CO₂ in modulating
46 GPP when there is a greater de-coupling between changes in CO₂ and climate. The contrast
47 between glacial and interglacial states during the Late Quaternary offers an ideal opportunity
48 to separate the impact of these two factors on vegetation. Glacial-interglacial shifts in climate
49 are largely driven by changes in orbital configuration which resulted in changes in the seasonal
50 and latitudinal patterns of incoming solar radiation (Berger, 1978; Berger and Loutre, 1991).
51 The Last Glacial Maximum (LGM), ca 21,000 years ago, had an orbital configuration similar
52 to the present but was characterised by the presence of large continental ice sheets and generally
53 colder and drier climates (Kageyama et al., 2021). The CO₂ level was ca 190 ppm, which is
54 close to the minimum for effective C₃ plant operation (Gerhart and Ward, 2010). The mid-
55 Holocene (MH), ca 6000 years ago, was characterised by a significantly different seasonal and
56 latitudinal distribution of incoming solar radiation (a result of changes in obliquity and
57 precession) which affected light availability for photosynthesis and produced warmer summers
58 in the northern hemisphere and wetter conditions in the sub-tropics (Brierley et al., 2020).
59 However, ambient CO₂ was only ca 264 ppm (Otto-Bleisner et al., 2017), somewhat lower than
60 the pre-industrial (PI) period (285 ppm) and considerably lower than today.

61 [Three sets of factors could potentially impact vegetation productivity changes between the](#)
62 [LGM, MH and pre-industrial periods: changes in climate, atmospheric CO₂ and solar radiation.](#)
63 [Several published studies have simulated LGM climate impacts on vegetation \(and/or fire,](#)
64 [interacting with vegetation\), with – or without – consideration of the additional physiological](#)
65 [effects of low CO₂ on plants \(Levis et al. 1999, Harrison and Prentice 2003, Martin Calvo et](#)
66 [al. 2014\). Other studies have performed factorial experiments to more formally separate the](#)
67 [effects of climate and CO₂ \(Woillez et al. 2011, O’ishi & Abe-Ouchi 2013, Claussen et al.](#)
68 [2013, Martin Calvo & Prentice 2015, Chen et al. 2019, Haas et al. 2023\).](#)

69 [Comparison among these studies of LGM-to-recent primary production shifts is approximate](#)
70 [at best because they have used different climate models and experimental protocols. Some have](#)
71 [used pre-industrial conditions as a reference; others, modern \(higher-CO₂\) conditions.](#)
72 [However, they all have used land ecosystem models based on the plant functional type \(PFT\)](#)
73 [concept. Uncertainty in the delimitation of PFTs and the parameter values assigned to them is](#)
74 [endemic to this type of model, as variation of quantitative traits within PFTs in the real world](#)
75 [is generally much larger than variation between them \(Kattge et al., 2011\). In some cases, the](#)
76 [model PFT representation has resulted in an unrealistic simulation of LGM vegetation patterns](#)

(e.g. Woiliez et al. 2011). Here we use the P model (Stocker et al. 2020), which accounts for acclimation and adaptation to environment independently of PFTs on the basis of universal eco-evolutionary optimality (EEO) hypotheses. The P model has been subject to extensive evaluation against worldwide data from eddy covariance flux towers across all biomes. We include an extension of the P model which simulates foliage cover and its seasonal cycle – also independently of PFTs. This extended model has been shown to reproduce foliage amounts and seasonal dynamics more accurately than any state-of-the-art vegetation model (Zhou et al. 2025). We use a simple process-based scheme to represent the relative competitive success of C₃ versus C₄ plants, which has been validated against worldwide soil carbon stable isotope data (Lavergne et al., 2024). This combination of three independently tested, PFT-independent modelling components enables us, for the first time, to apply an EEO-based approach to simulate LGM and recent vegetation function in a globally uniform way

There has been some work on the implications of MH climate for biome distributions (e.g. Kaplan et al., 2003; Wohlfahrt et al., 2008) but little consideration of the impacts of climate and CO₂ on global productivity changes since the MH (Foley, 1994; François et al. 1999). Here, we use the same consistent methodology that we apply to the LGM to estimate MH-to-pre-industrial changes in global GPP. Our analysis includes the effect of changes in the light regime, which are a necessary consequence of changes in the seasonal and latitudinal distribution of insolation due to orbital forcing, as well as changes in cloud cover linked to monsoon shifts.

EEO-based modelling approaches provide parameter-sparse representations of plant and vegetation processes, thus considerably reducing uncertainties due to model parameterisation (Harrison et al. 2021). They have been shown to perform as well or better than more complex models under recent conditions (Cai et al., 2025; Zhou et al., 2025) and thus can provide a robust way of modelling vegetation changes under different climate regimes. We use a series of counter-factual experiments to examine the magnitude of changes due to individual drivers (climate parameters, solar radiation and CO₂) on the simulated GPP and to determine the regions where specific factors are most influential.

2 Methods

2.1 Modelling Scheme

We simulated vegetation changes at the LGM and the MH compared to the pre-industrial (PI) state using a sequence of linked models that predict GPP, leaf area index (LAI) and C₃/C₄ competition based on EEO theory (Fig. 1).

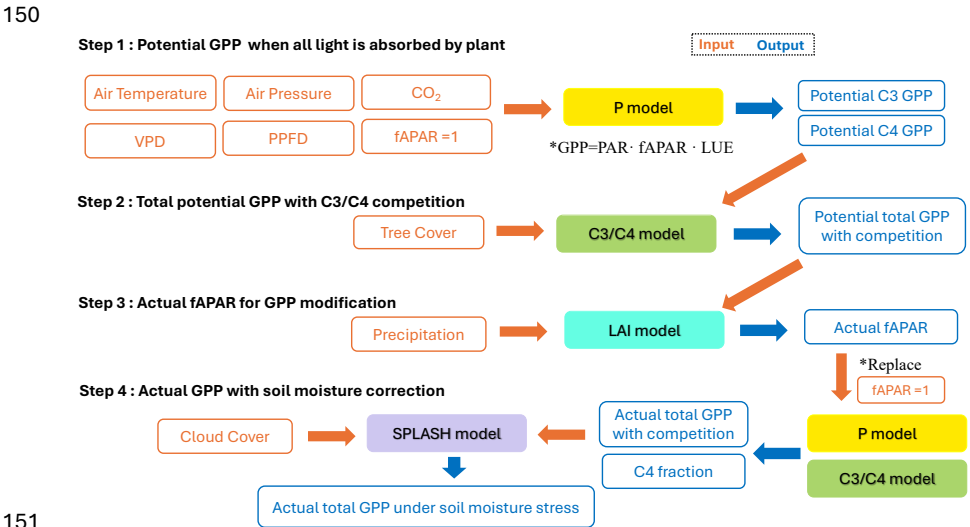
The P model (Wang et al., 2017, Stocker et al., 2020) is a light-use efficiency model that simulates GPP. It uses the Farquhar-von Caemmerer-Berry photosynthesis model (Farquhar et al., 1980) for instantaneous biochemical processes combined with two EEO hypotheses describing photosynthetic acclimation, the ‘coordination’ and ‘least-cost’ hypotheses (Prentice et al., 2014, Wang et al., 2017), to account for the spatial and temporal acclimation of carboxylation and stomatal conductance to environmental variations at weekly to monthly time scales. Although the P model simulates both C₃ and C₄ photosynthesis, it does not need to make any other distinctions between plant functional types. The required inputs to the model (Fig. 1) are air temperature (°C), vapour pressure deficit (VPD, Pa) derived from relative humidity, air pressure (Pa) (to account for the effect of elevation on photosynthesis, incident photosynthetic photon flux density (PPFD, $\mu\text{mol m}^{-2} \text{s}^{-1}$) estimated from short wave solar radiation, and

Formatted: Space Before: Auto

Deleted: Previous work on the impact of low CO₂ on vegetation at the LGM has focused mainly on the implications for tree cover (e.g. Harrison and Prentice, 2003; Prentice et al., 2011; Bragg et al., 2013; Martin Calvo and Prentice, 2015) rather than vegetation productivity. There has been work on the implications of MH climate for vegetation patterns (e.g. Kaplan et al., 2003; Wohlfahrt et al., 2008), but there has been little consideration of the impact of climate and CO₂ on overall productivity during this period. The role of changes in solar radiation for photosynthesis has not been examined in either period. In this study, we use an eco-evolutionary optimality (EEO) based modelling approach to investigate the relative importance of climate, solar radiation and CO₂ changes on the respective contributions of C₃ and C₄ plants to total GPP, focusing on the LGM and MH states compared to a pre-industrial baseline.

Formatted: Font colour: Auto

138 ambient CO₂ concentration. The P model has been extensively validated and shown to predict
 139 the geographic patterns of GPP under modern conditions successfully (Wang et al., 2017;
 140 Stocker et al., 2020). Furthermore, it correctly predicts related physiological characteristics,
 141 including the global pattern of the maximum carboxylation (V_{cmax}) rate in relation to gradients
 142 in PPFD, temperature and VPD (Smith et al., 2019), the seasonal variation of V_{cmax} in different
 143 biomes (Jiang et al., 2020), its response to atmospheric CO₂ (Smith and Keenan, 2020), and
 144 the variation of photosynthetic traits along elevational gradients (Peng et al., 2020). The
 145 responses of photosynthetic properties to enhanced CO₂ as simulated by the P model have been
 146 validated against both Free Air Carbon dioxide Enrichment (FACE) experiments (Wang et al.,
 147 2017) and controlled-environment experiments (Smith and Keenan, 2020). Moreover, the
 148 model's implied response of photosynthetic capacity to CO₂ has been validated by
 149 measurements on plants experimentally grown at low (160 ppm) CO₂ (Harrison et al., 2021).



151
 152 **Figure 1: Flowchart showing the steps in the modelling procedure.**

154 The P model simulates potential GPP for C₃ and C₄ plants separately (Figure 1). These
 155 estimates were fed into a simple model of C₃/C₄ competition based on the P model (Lavergne
 156 et al., 2024). The relative advantage of C₄ plants is estimated as the difference between the
 157 monthly potential GPP for C₃ and C₄ plants, summed over the year. The C₄ share of total GPP
 158 was then estimated by fitting a logistic curve between the model estimated C₄ relative
 159 advantage and observed C₄ abundance. These calculations assume that neither water nor
 160 nutrients are limiting growth. However, under these conditions, C₃ trees out-compete C₄
 161 grasses through shading, even where the C₄ pathway would yield higher rates of
 162 photosynthesis. The model accounts for this using an additional function relating the proportion
 163 of GPP from trees to total potential GPP based on a power function for the relationship between
 164 prescribed annual mean percentage tree cover and the simulated annual GPP of C₃ plants. Thus,
 165 tree cover is an additional required input to the competition model (Figure 1). The competition
 166 model also uses a minimum temperature threshold to define conditions under which C₄ plants
 167 cannot grow, where this limit is set to a minimum temperature of the coldest month of −24°

169 based on experimental data. The competition model has been shown to reproduce global
170 patterns in the relative abundance of C₃/C₄ plants as well as the observed rate of $\Delta^{13}\text{C}$ in recent
171 decades, as shown by independent atmospheric estimates (Lavergne et al., 2020).

172 To convert potential GPP to actual GPP, we used an LAI model (Figure 1) that predicts the
173 seasonal cycle of LAI based on environmental conditions and an estimate of the potential GPP,
174 i.e. the GPP predicted when the fraction of absorbed photosynthetically active radiation,
175 fAPAR, is set to 1 (Zhou et al., 2025). The seasonal LAI is calculated using a moving average
176 to represent the time lag between allocation to leaves and modelled steady-state LAI. A
177 seasonal maximum fAPAR model was embedded in this model to limit seasonal LAI
178 predictions (Zhu et al., 2022; Cai et al., 2025). The calculation of seasonal maximum fAPAR
179 incorporates a water-carbon trade-off: it is defined as the lesser of an energy-limited
180 (maximising GPP) and a water-limited (maximising the use of available precipitation) estimate
181 (Zhu et al., 2022; Cai et al., 2025). The seasonal LAI is calculated using a moving average to
182 represent the time lag between allocation to leaves and modelled steady-state LAI. The model
183 has been shown to capture observed LAI dynamics across all biomes at different temporal
184 scales (weekly, seasonal, annual and interannual variability) both at individual eddy-covariance
185 flux measurement sites and when compared to satellite-derived LAI (Zhou et al., 2025).
186 Furthermore, it predicts both the multi-year average LAI and the annual trends in LAI better
187 than the biosphere models used in the Trends and Drivers of Terrestrial Sources and Sinks of
188 Carbon Dioxide (TRENDY) project (Zhou et al., 2025). The seasonal cycle of fAPAR is
189 calculated from the seasonal cycle of LAI using Beer's law (Swinchart, 1962) and this is then
190 used to calculate seasonal changes in actual GPP. Finally, we apply an empirical soil moisture
191 correction ($\beta(\theta)$; Stocker et al., 2020) to account for the impact of soil moisture stress on GPP,
192 using the Simple Process-Led Algorithms for Simulating Habitats (SPLASH) model (Davis et
193 al., 2017).

Deleted: 3

Deleted: 3

Deleted: The model has been shown to capture LAI dynamics across biomes, both at individual eddy-covariance flux measurement sites and spatial patterns (Zhou et al., 2025).

194 2.2. Derivation of LGM, MH and PI climate inputs

195 We use LGM, MH and pre-industrial (PI) climate simulations (Supplementary Table 1) run
196 using the low-resolution version of the Max Planck Institute Earth System Model (MPI-
197 ESM1.2-LR; Mauritsen et al., 2019; doi:10.22033/ESGF/CMIP6.6642) made as part of the
198 fourth phase of the Palaeoclimate Modelling Intercomparison Project (PMIP4; Kageyama et
199 al., 2017; Otto-Bleisner et al., 2019). This model is amongst the best performing of the PMIP
200 models when evaluated using reconstructions of land and ocean climates (Brierley et al., 2020;
201 Kageyama et al., 2021) and uniquely has archived all the necessary outputs needed to run the
202 EEO-based models (Fig. 1). The experiments were run following the PMIP4 protocols for each
203 time period (Kageyama et al., 2017; Otto-Bleisner et al., 2019). The PI experiment was run for
204 1000 years using modern ice sheet and land-sea configurations and a CO₂ level of 284.3 ppm
205 (SI Table 1). The MH experiment uses the same ice sheet and land-sea configurations as the PI
206 but uses appropriate changes in orbital parameters and a CO₂ level of 264.4 ppm (SI Table 1).
207 The MPI-ESM1.2-LR LGM experiment uses the ICE6G_C ice sheet and corresponding
208 modification in land-sea geography, appropriate orbital parameters and a CO₂ level of 190 ppm
209 (SI Table 1). The LGM simulation was re-started from a previous LGM simulation and then
210 spun-up for 3850 years.

211 The MPI-ESM1.2-LR model has a spectral resolution of T63 (192 x 96 longitude/latitude). The
212 outputs necessary to run the EEO-based models were down-scaled to a resolution of 0.5° using
213 spline interpolation. The daily data necessary to run the EEO-based models was obtained from
214 monthly data, also using nearest neighbour and bilinear interpolation. Although many previous

vegetation modelling studies have used climate anomalies from a baseline experiment (e.g. LGM minus PI), here we used model outputs directly – because although the anomaly approach is well-suited to adjust climate variables, it cannot be used to adjust simulated tree cover.

2.3. Stein-Alpert decomposition

Climate, light availability and atmospheric CO₂ concentration have independent effects on plant growth. To evaluate the unique effects of these different factors, and potential synergies between them, on the changes in GPP between the PI and the LGM and MH experiments, we used the Stein-Alpert decomposition method (Stein and Alpert, 1993), an approach that has been previously shown to be useful in evaluating the impacts of different factors on past vegetation changes (e.g. Martin-Calvo and Prentice, 2015; Sato et al., 2021). We used the pre-industrial simulation as the reference case (f₀) and ran a series of factorial experiments in which specific factors were changed to their LGM or MH conditions as follows:

Experiment f1: LGM (or MH) climate, PI CO₂ and PPFD
 Experiment f2: LGM (or MH) CO₂, PI climate and PPFD
 Experiment f3: LGM (or MH) PPFD, PI climate and CO₂
 Experiment f12: LGM (or MH) climate and CO₂, PI PPFD
 Experiment f13: LGM (or MH) climate and PPFD, PI CO₂
 Experiment f23: LGM (or MH) CO₂ and PPFD, PI climate
 Experiment f123: LGM (or MH) climate, CO₂ and PPFD

The impact of each factor or combination of factors was then calculated as:

$$\begin{aligned} \langle f1 \rangle &= f1 - f0 \\ \langle f2 \rangle &= f2 - f0 \\ \langle f3 \rangle &= f3 - f0 \\ \langle f12 \rangle &= f12 - (f1 + f2) + f0 \\ \langle f13 \rangle &= f13 - (f1 + f3) + f0 \\ \langle f23 \rangle &= f23 - (f2 + f3) + f0 \\ \langle f123 \rangle &= f123 - (f12 + f13 + f23) + (f1 + f2 + f3) - f0 \end{aligned}$$

where the first three experiments represent the influence of the single changed factor, the second three experiments represent synergies between pairs of factors, and the final experiment represents the three-way synergy between all three factors.

The comparisons can only be made for the common land area between the PI and each palaeoclimate experiment. The LGM factorial experiments therefore have a baseline GPP value for the f₀ experiment that does not include the areas exposed by lowered sea level, although these are considered in the full LGM experiment. The full LGM and MH experiments include changes to both air pressure and tree cover; these are not considered in the factorial experiments because preliminary analyses indicated that the impact of these changes on simulated global GPP was less than 0.2PgC yr⁻¹ and therefore negligible.

3. Results

Simulated global GPP at the LGM was 83.9 PgC yr⁻¹ (Table 1), considerably lower than the simulated global value during the pre-industrial period (109.6 PgC yr⁻¹). The largest reductions in GPP compared to the pre-industrial baseline were in the northern hemisphere extra-tropics

Formatted: Superscript

(Figure 2, Table 2), which experienced a more than 50% reduction in GPP. There was a more modest decrease (13%) in the southern extra-tropics and only a small decrease in the tropics (3%). Part of the reduction (10.5 PgC yr⁻¹) in global GPP reflects the loss of vegetation from areas that were covered by ice at the LGM; this was only partially compensated by vegetation growth on the continental shelves exposed by the reduced sea level (8.3 PgC yr⁻¹). Although there was a reduction overall and across most of the world, some regions experienced a small increase in productivity at the LGM compared to the PI (Figure 3). These are all in now-arid regions and the increase therefore presumably reflects the fact that moisture constraints on vegetation growth were reduced in the colder climate of the LGM.

Table 1: Contribution to global changes in gross primary production (GPP) in the Last Glacial Maximum (LGM), the mid-Holocene (MH), and the pre-industrial (PI) experiments. The table gives the global total in each experiment, the GPP of land exposed by lowered sea level at the LGM, the GPP of land that was covered by ice sheets at the LGM and was exposed in the MH and PI experiments, and GPP for the land area in common between all three experiments.

	Total non-glaciated land area	Land area covered by ice at LGM	Land area exposed by lowered sea level at LGM	Common land area between the experiments
GPP LGM	83.9 PgC yr ⁻¹	n/a	8.3 PgC yr ⁻¹	75.5 PgC yr ⁻¹
GPP MH	110.3 PgC yr ⁻¹	10.6 PgC yr ⁻¹	n/a	99.6 PgC yr ⁻¹
GPP PI	109.6 PgC yr ⁻¹	10.5 PgC yr ⁻¹	n/a	99.1 PgC yr ⁻¹

Table 2: Regional contributions to total annual gross primary production (GPP) in the tropics, the northern extra-tropics (NET) and the southern extra-tropics (SET) in the Last Glacial Maximum (LGM), the mid-Holocene (MH), and the pre-industrial (PI) experiments.

	LGM	MH	PI
Tropics (25°N-25S)	56.4 PgC yr ⁻¹	57.7 PgC yr ⁻¹	58.3 PgC yr ⁻¹
NET (>25°N)	21.4 PgC yr ⁻¹	46.2 PgC yr ⁻¹	44.3 PgC yr ⁻¹
SET (>25°S)	6.0 PgC yr ⁻¹	6.4 PgC yr ⁻¹	6.9 PgC yr ⁻¹

Simulated GPP increased to 110.3 PgC yr⁻¹ in the MH compared to 83.9 PgC yr⁻¹ at the LGM. Part of this increase (10.6 PgC yr⁻¹) was a result of vegetation growth in areas that were covered by ice sheets during the LGM. However, there were notable increases in the non-glaciated high latitudes (northern Siberia and Beringia), in tropical regions, and in areas influenced by MH monsoon expansion (Sahel, south-east Asia, southern African savannas and the South American cerrado) (Figure 2). GPP increased in the common area between the LGM and MH experiments by ca 32% (Table 1), with the largest increase in the NET (Table 2). The transition from the MH to the PI resulted in a very small decrease in global GPP (Figure 3). Simulated GPP in the MH was slightly higher (4%) than in the PI experiment in the northern extra-tropics, although still lower than in the PI in other regions (Table 2).

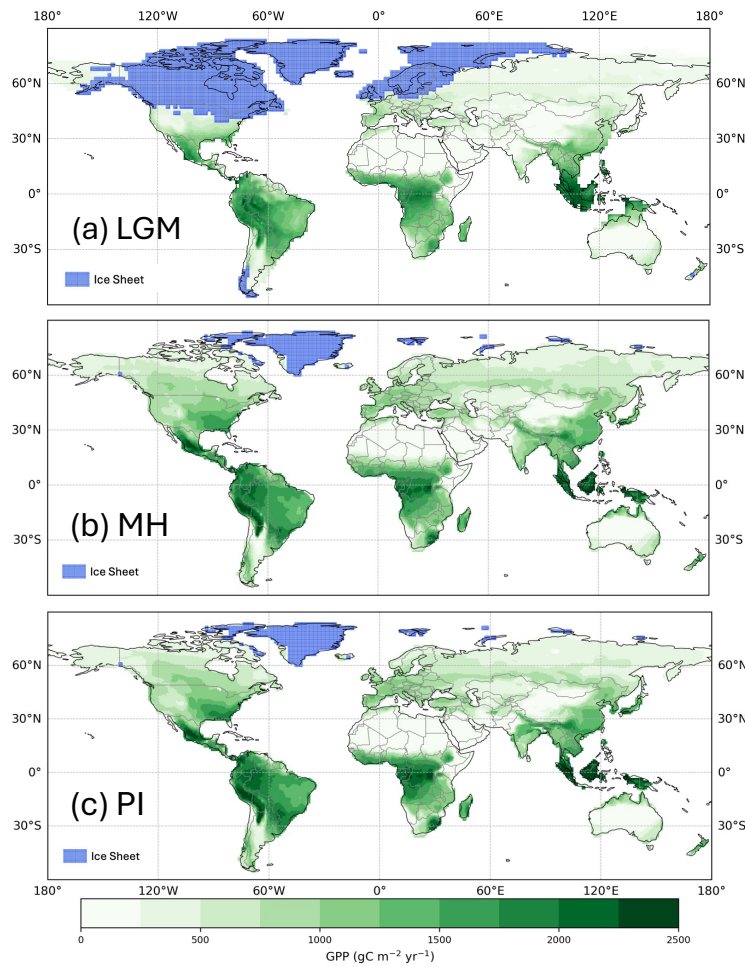


Figure 2: Simulated total annual gross primary production (GPP). The plots show simulated GPP for (a) the Last Glacial Maximum (LGM), (b) the mid-Holocene (MH), and (c) the pre-industrial (PI).

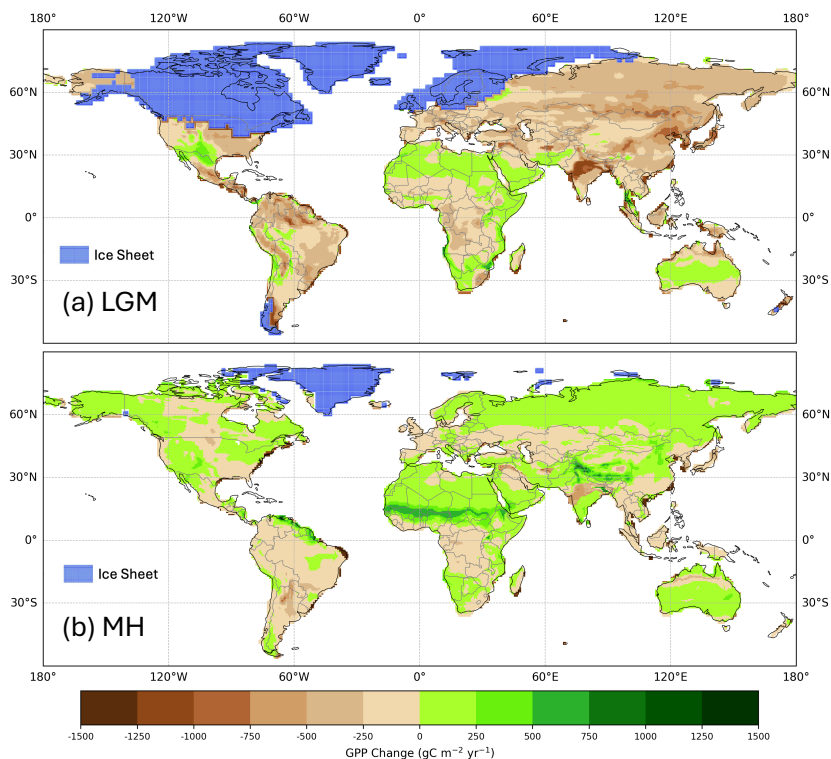


Figure 3: Simulated change in total annual gross primary production (GPP) between the pre-industrial (PI) and (a) the Last Glacial Maximum (LGM) and (b) the mid-Holocene (MH).

These changes in GPP were accompanied by a shift in the relative importance of C₃ and C₄ plants (Table 3, Figure 4). C₄ plants represented 23% and 25% of the vegetation fraction in the PI and MH experiments respectively, but 40% of the vegetation fraction at the LGM. C₄ plants were responsible for 56% of the total GPP at the LGM compared to 25% and 21% in the MH and PI respectively. The fraction of C₄ plants increased across most regions of the world at the LGM (Supplementary Figure 1), but in some regions including the Central Great Plains of North America, the northern Sahel, and the Tibetan Plateau and part of the Loess Plateau in northeastern China C₄ plants were less abundant than in the PI. The areas where C₄ plants were less abundant in the MH than in the PI were more extensive (Supplementary Figure 1) and are primarily in regions of northern Africa and Asia influenced by the expansion of the monsoons.

Table 3: Changes in C₃/C₄ fraction and contribution of C₃/C₄ vegetation to total GPP

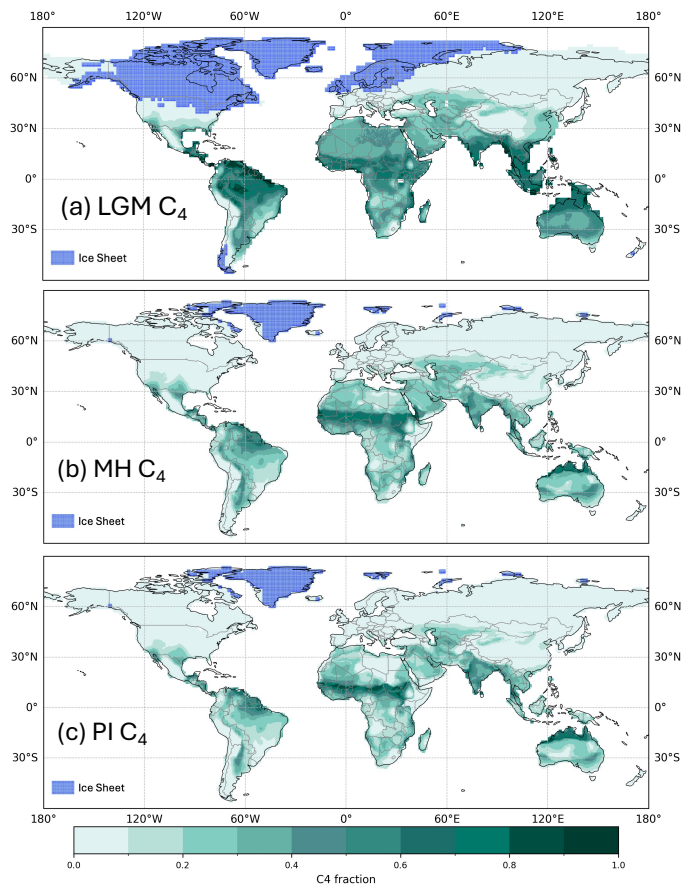
	LGM	MH	PI
Global average C ₄ fraction	40%	25%	23%
Global average C ₃ contribution of total annual GPP (gC m ⁻² yr ⁻¹)	281.4	608.9	618.6
Global C ₃ contribution to total GPP (PgC yr ⁻¹)	37.1	82.8	86.2
Global average C ₄ contribution of total annual GPP (gC m ⁻² yr ⁻¹)	297.7	166.3	140.5
Global C ₄ contribution to total GPP (PgC yr ⁻¹)	46.8	27.5	23.4

Formatted Table

Formatted: Superscript

Formatted: Superscript

Deleted: m² yr



324 **Figure 4.** Global C_4 fraction distribution for (a) the Last Glacial Maximum (LGM), (b) the
325 mid-Holocene (MH), and (c) the pre-industrial (PI).
326

327 The factorial experiments showed that the changes in climate and CO_2 had a large negative
328 effect on GPP at the LGM, while light (PPFD) had a small positive effect (Table 4, Figure 5).
329 The shift to a colder, drier climate had a somewhat larger negative effect on plant productivity
330 ($-14.8 \text{ PgC yr}^{-1}$) than the reduction in CO_2 ($-12.2 \text{ PgC yr}^{-1}$). Climate has a major impact on
331 reducing GPP in the high- to mid-latitudes of North America and Eurasia (Figure 6a,
332 Supplementary Figure 2) but changes due to the lowering of CO_2 were almost as important
333 (Figure 6b, Supplementary Figure 3). Changes in climate (Supplementary Figure 2;
334 [Supplementary Table 2](#)), most likely the overall reduction in precipitation (Supplementary
335 Figure 5), was the most important factor causing reduced GPP in northern Amazonia, India

336 and north-western China. However, the cooler climate had a positive effect on GPP in regions
337 that are semi-arid today (Supplementary Figure 2, Supplementary Figure 5). Changes in PPFD
338 were the dominant factor in increasing GPP at the margin at the northernmost edge of the
339 vegetated zone downwind of the Scandinavian ice sheet and into Beringia (Supplementary
340 Figure 4).

341 The two-way synergy between climate and CO₂ was positive (Table 4, Figure 5), i.e. the change
342 in GPP is less than would be expected if the impacts were additive. This reflects the fact that,
343 whereas lower temperatures favour C₃ plants, lower CO₂ offsets this and promotes the
344 expansion of C₄ plants over much of the globe (Supplementary Figures 6, 7). C₄ plants were
345 especially favoured in tropical regions, where the climate changes were relatively muted, and
346 the changes in CO₂ correspondingly more influential. The synergies of both climate and CO₂
347 with PPFD, although small (0.9 and 0.2 PgC yr⁻¹ respectively) are negative. The synergy
348 between climate and PPFD probably reflects the fact reduced cloud cover in drier climates
349 (Supplementary Figure 6, 8). The synergy between CO₂ and PPFD stems from the fact that
350 both low CO₂ and high PPFD favour C₄ plants, increasing GPP particularly in the extratropics
351 (Supplementary Figure 7, 8).

352 Climate changes had a positive effect on GPP in the mid-Holocene (Table 4, Figure 5). This
353 likely reflects the impact of increased precipitation in now semi-arid regions due to monsoon
354 expansion combined with warmer growing seasons in the high northern latitudes, both
355 consequences of the orbitally-induced changes in solar radiation (Supplementary Figure 5).
356 These experiments also show that changes in PPFD have a positive effect on plant growth,
357 particularly in the northern mid- to high latitudes and in now-arid regions (Supplementary
358 Figure 4). The positive impact in northern mid- to high latitudes appears to be due to
359 enhancement of growing season conditions for C₃ plants, while the positive impact in now-arid
360 regions reflects an increase in C₄ plants (Supplementary Figure 8). However, the reduction of
361 CO₂ compared to the PI state (16 ppm) resulted in a much larger overall reduction in GPP than
362 the enhancements due to climate or PPFD changes (Supplementary Figure 3). The impact of
363 the lower CO₂ in the mid-Holocene is the dominant factor causing reductions in GPP in
364 southern China, the southern hemisphere tropical and savanna regions in Africa, and in the
365 cerrado of South America (Figure 6). The two-way synergies between the three drivers are all
366 positive, but small (Table 4, Figure 5).

Table 4. Stein-Alpert decomposition of the impact of changes in climate, CO₂ and light (photosynthetic photon flux density, PPFD), and their synergies, on gross primary production (GPP) at the Last Glacial Maximum (LGM) and in the mid-Holocene (MH) compared to the pre-industrial (PI) simulations. Note that the baseline GPP value for the LGM is for the common land area between this experiment and the PI simulation and is therefore smaller than the baseline GPP value for the MH decomposition.

Experiment	Stein-Alpert decomposition	Climate	CO ₂	PPFD	GPP (PgC _{yr} ⁻¹)
LGM	f0	PI	PI	PI	99.1
	f1, LGM	LGM	PI	PI	84.3
	f2, LGM	PI	LGM	PI	86.9
	f3, LGM	PI	PI	LGM	100.3
	f12, LGM	LGM	LGM	PI	75.4
	f13, LGM	LGM	PI	LGM	84.6
	f23, LGM	PI	LGM	LGM	87.8
	f123, LGM	LGM	LGM	LGM	75.7
MH	f0	PI	PI	PI	109.6
	f1, MH	MH	PI	PI	111.5
	f2, MH	PI	MH	PI	107.0
	f3, MH	PI	PI	MH	110.6
	f12, MH	MH	MH	PI	109.1
	f13, MH	MH	PI	MH	112.5
	f23, MH	PI	MH	MH	108.1
	f123, MH	MH	MH	MH	110.1

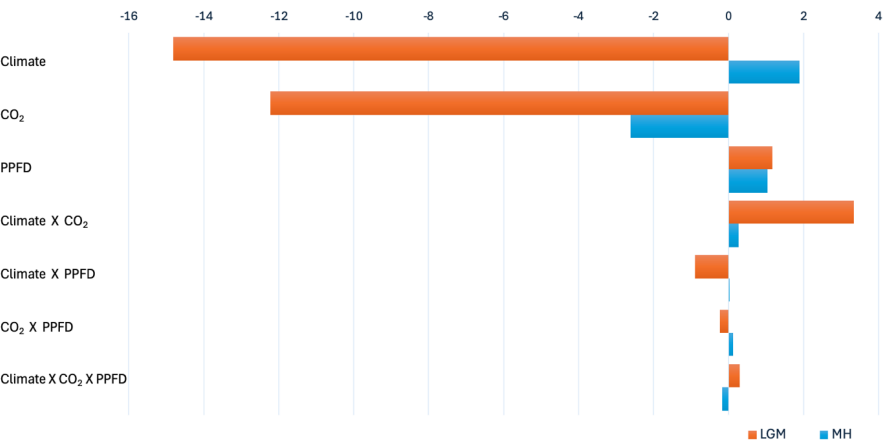
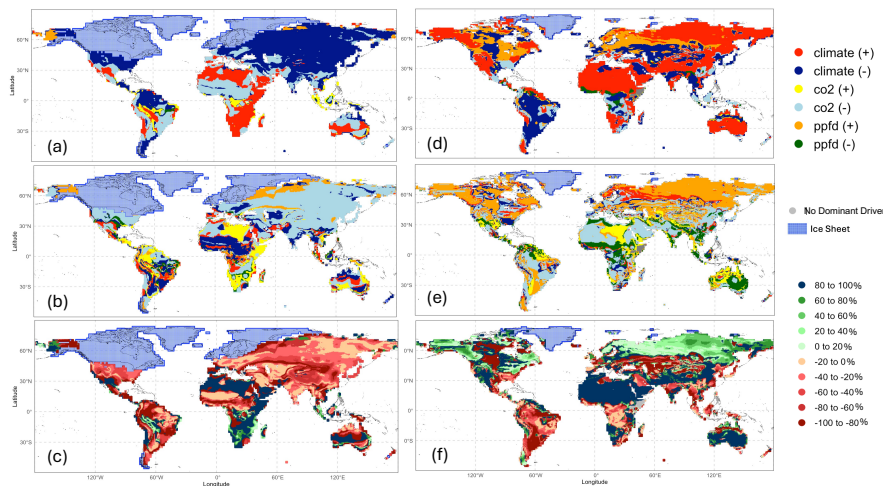


Figure 5. Impact of climate, light and CO₂ on the changes in gross primary production (GPP, PgC) at the Last Glacial Maximum (LGM) and the mid-Holocene (MH) compared to the pre-industrial (PI) period. Note that the results are based on the common land area between each experiment and the PI simulation.

383



384
385 *Figure 6. Global distribution of (a) main drivers and constraints (b) secondary drivers and*
386 *constraints and (c) the proportional difference (percentage) of total change between the main*
387 *and the secondary driver on gross primary production (GPP) at the Last Glacial Maximum*
388 *(LGM) compared to the pre-industrial (PI) experiment; and (d) main drivers and constraints*
389 *(e) secondary drivers and constraints (f) the proportional difference (percentage) of total*
390 *change between the main and the secondary driver on gross primary production (GPP) in the*
391 *Mid-Holocene (MH) compared to the pre-industrial (PI) experiment.*

392
393 **4. Discussion**

394 We have shown that the LGM was characterised by a large reduction in modelled GPP, while
395 the mid-Holocene was characterised by a small increase in GPP compared to the pre-industrial
396 state. The simulated reduction at the LGM is consistent with previous model-based estimates
397 (e.g. Francois et al., 1998; Prentice et al., 2011; Hoogakker et al., 2016), including those from
398 the latest phase of the Couple Model Intercomparison project (CMIP6/PMIP4: Supplementary
399 Table 3). However, there is a considerable range in the magnitude of these modelled estimates,
400 reflecting differences in both the simulated LGM climate and in the vegetation model used.
401 Our estimate of the GPP at the LGM (84 PgC yr⁻¹) is in the middle of the range of the
402 CMIP6/PMIP4 models (61-109 PgC yr⁻¹). There have been a limited number of studies that
403 have estimated GPP at the LGM by constraining model estimates using oxygen isotope records
404 from ice core (Landais et al., 2007; Ciais et al., 2011; Yang et al., 2022). These show a similarly
405 large range in simulated GPP (40-110 PgC yr⁻¹), in part because of the uncertainties associated
406 with estimating ocean productivity and respiration fractionation rates. Thus, although there is
407 a consensus that GPP was considerably lower at the LGM than during pre-industrial times, and
408 this is consistent with pollen evidence for a very large reduction in tree cover over much of the
409 world (Prentice et al., 2000; Williams, 2003; Pickett et al., 2004; Marchant et al., 2009), the
410 absolute magnitude of this change is uncertain. Nevertheless, since the climate simulated by
411 the MPI ESM has been shown to reproduce pollen-based climate reconstructions better than
412 most other CMIP6/PMIP4 models (Kageyama et al., 2021) and we use robust EEO-models to
413 estimate the change in GPP, the partitioning of the impacts of different factors in the simulated
414 reduction of GPP is likely to be robust.

The modelled abundance of C₄ plants was nearly double at the LGM compared to the pre-industrial era (40% versus 23% of the vegetation fraction) and that C₄ vegetation was responsible for 56% of the total modelled GPP at that time. These changes are broadly consistent with pollen-based reconstructions, indicating a substantial reduction in tree cover at the LGM (Prentice et al., 2000). However, while pollen data can be used to discriminate between trees (virtually all C₃) and grasses, it cannot be used to infer changes in the importance of C₃ and C₄ grasses. Compound-specific $\delta^{13}\text{C}$ analyses of leaf wax biomarkers provide evidence of the relative contribution of C₃ and C₄ plants (Eglinton & Eglinton, 2008; Diefendorf et al., 2010) and have shown that C₄ plants were more abundant at the LGM than during the Holocene in many regions of the world (e.g. in southern Africa: Rommerskirchen et al., 2006; Vogts et al., 2012; eastern Africa: Sinninghe Damsté et al., 2011; Himalayan Basin: Galy et al., 2008; southern China: Jiang et al., 2019; south-western North America: Cotton et al., 2016; northern South America: Makou et al., 2007), consistent with our simulations. There are a few regions where C₄ plants were less abundant at the LGM than during the Holocene, including the Chinese Loess Plateau and the Great Plains of North America (Cotton et al., 2016). Both of these regions are identified as characterised by reduced C₄ abundance in our simulations. A number of modelling studies have shown that C₄ plants were globally more abundant at the LGM (e.g. Harrison & Prentice, 2003; Bragg et al., 2013; Martin Calvo & Prentice, 2015) but did not quantify the relative contribution of C₄ plants to global GPP. Thus, our analyses are consistent with previous studies of the nature of the shift in vegetation composition at the LGM and provide, for the first time, a quantitative estimate of the magnitude of this change.

Climate has a negative effect on GPP at the LGM but a positive effect in the MH. The LGM climate was globally colder and drier, although the largest changes in both temperature and precipitation were in the northern mid- to high-latitudes (Kageyama et al., 2021). This is reflected in our simulations; the overall reduction in GPP compared to the pre-industrial baseline in the northern extra-tropics was 52%, far larger than the reductions in the southern extra-tropics (13%) or the tropics (3%). The cooling in the ice-free regions of the northern extra-tropics reflects advection of cold air temperatures downwind from the ice sheets, while the drying largely reflects the temperature-induced reduction in evaporation and precipitation recycling (Izumi et al., 2013; Li et al., 2013; Kageyama et al., 2021). The positive effect of climate on GPP in the MH reflects changes in precipitation in now semi-arid regions of the sub-tropics as a result of the expansion of the northern hemisphere monsoons and a lengthening of the growing season in the northern mid- to high-latitudes as a result of increased solar radiation in summer (Brierley et al., 2020). These changes in climate are reflected in our simulations; although the northern extra-tropics are the only region to show an overall increase in GPP compared to the pre-industrial (4%), regions influenced by monsoon expansion, such as the Sahel and parts of Asia, also show increased GPP.

The modelled reduction of GPP by low LGM relative to pre-industrial CO₂ was of similar magnitude (12%) to that of LGM climate (15%). Some other factorial model experiments (e.g. O’Ishi and Abe-Ouchi, 2013; Claussen et al., 2013; Martin Calvo and Prentice, 2015; Chen et al., 2019; Haas et al., 2023; see Supplementary Table 4) have shown a larger impact of CO₂ on primary production (either GPP or net primary production, NPP) relative to climate. For example, Claussen et al. (2013) showed reductions in NPP of 4% due to climate and 45% due to CO₂ and Martin Calvo and Prentice (2015) showed reductions in NPP of 2% due to climate and 23% due to CO₂. Some of differences among experiments may have been caused by difference in modelled climate (Haas et al., 2023); but changes in PFT abundance are likely to be an important additional source of uncertainty. Woillez et al. (2011) also indicate a dominant role for low glacial CO₂ in reducing NPP at the LGM. In that analysis, however, a greater

sensitivity of needleleaf PFTs to low CO₂ compared to broadleaf PFTs was implied by choices of parameter values that were not necessarily well-founded, and led to an unrealistically large simulated extent of broad-leaved forests at the LGM.

In addition to the fact that these various experiments were based on different models of the LGM climate, they were also made using different biosphere models (Supplementary Table 4) – which may have different sensitivities to CO₂ changes. Thus, although models agree that changes in CO₂ contributed to the large observed differences between LGM and pre-industrial vegetation patterns, the magnitude of the impact of low CO₂ on primary production is still uncertain. The modelled impact of lowered CO₂ on GPP in the MH here is larger than the impact of climate, offsetting the positive impacts of climate change in the MH experiment. The importance of CO₂ in driving vegetation changes has been widely commented on for the LGM (Polley et al., 1993; Jolly & Haxeltine, 1997; Cowling & Sykes, 1999; Harrison & Prentice, 2003; Flores et al., 2009; Prentice et al., 2011; Bragg et al., 2013; Martin Calvo & Prentice, 2015) and in the context of ongoing and future climate changes (Piao et al., 2006; Keenan et al., 2014; Archer et al., 2017; Haverd et al., 2020; Piao et al., 2020) but its role in offsetting the positive impacts of climate change in the MH has not been widely noted. The simulated overall change in GPP in the MH compared to the PI is small (< 1 PgC yr⁻¹). Nevertheless, the changes in response to individual drivers are consistent with expectations: changes in climate and PPFD had a positive impact on GPP while the reduction in CO₂ in the MH compared to the PI had a negative impact on GPP. The positive effect of climate on GPP in the MH reflects changes in precipitation in now semi-arid regions of the sub-tropics, as a result of the orbitally induced expansion of the northern hemisphere monsoons and the lengthening of the growing season in the northern mid- to high-latitudes (Brierley et al., 2020). These changes in climate are reflected in our simulations. The northern extratropics are the only region to show an overall increase in GPP compared to the pre-industrial (4%) when CO₂ effects are included, but regions influenced by monsoon expansion, such as the Sahel and parts of South and East Asia, also show a tendency to increased GPP due to the MH climate.

We have derived climate inputs from the MPI ESM. When compared to reconstructions of both marine and terrestrial climate variables, the MPI ESM has been shown to be among the best-performing models both for the LGM and the mid-Holocene (Brierley et al., 2020; Kageyama et al., 2021). Nevertheless, the use of a single climate model is a limitation of this study. It would be useful to repeat these analyses with a wider range of models that have made palaeoclimate simulations of these two key periods, but the constraint is that most of these models do not provide information on changes in tree cover that is to run the C₃/C₄ competition model.

We have used a sequence of EEO-based models to simulate GPP and the relative contribution of C₃ and C₄ plants to overall productivity. Haas et al. (2023) also used the P model to simulate GPP at the LGM. Other studies of past vegetation changes have used models that simulate changes in past vegetation on the basis of the competition between PFTs. PFT-based models require key physiological parameters to be specified separately for each PFT. The EEO modelling approaches used here avoid this complexity, considerably reducing uncertainties due to model parameterisation (Harrison et al., 2021) while at the same time representing the key processes of photosynthesis and plant growth accurately (Wang et al., 2017; Smith et al., 2019; Jiang et al., 2020; Lavergne et al., 2020; Peng et al., 2020; Smith & Keenan, 2020; Wang et al., 2020; Xu et al., 2021; Zhu et al., 2022). Furthermore, they capture recent trends in vegetation growth more accurately than the land-surface models used to predict the terrestrial carbon cycle (Cai et al., 2025; Zhou et al., 2025).

Formatted: Normal (Web), Space Before: 0 pt

Deleted: The impact of lowered CO₂ on GPP is only slightly smaller than the changes caused by climate at the LGM, reinforcing the overall reduction of GPP at the LGM. The impact of lowered CO₂ on GPP in the MH is larger than the impact of climate, offsetting the positive impacts of climate change in the MH experiment.

Deleted: Despite the comparatively small change in CO₂ between the PI and MH (20 ppm), according to our simulations the lowering of CO₂ would have reduced GPP by ca 3 PgC whereas the increase produced by the change in climate is only 2 PgC.

521
522

5. Conclusions

523 Eco-evolutionary optimality approaches provide a robust way of modelling vegetation changes
524 under different climate regimes. We compared simulated changes in GPP and C_3/C_4 plant
525 abundance in a cold glacial and a warm interglacial period relative to the pre-industrial state.
526 We showed that the colder, drier climate at the LGM substantially decreases GPP and the
527 warmer, wetter climate of the MH increases GPP. Changes in vegetation productivity caused
528 by the lower CO_2 in both intervals compared to the pre-industrial contributed to the reduction
529 of GPP at the LGM and was sufficient to annul the positive impacts of climate on GPP during
530 the MH. These results point to the importance of a realistic treatment of the direct physiological
531 impacts of CO_2 on plant growth to simulate realistic ecosystem changes, both in the past and
532 in the future.

533 Data Availability

534 The CMIP6 MPI-ESM1-2-LR outputs are accessible via the Earth System Grid Federation
535 (ESGF) at <http://esgf-node.llnl.gov/search/cmip6/> (last accessed: 2 December 2024).
536 Interpolated input data and derived outputs related to this study are available at DOI:
537 10.5281/zenodo.14257604. The documentation for the P model, the C_3/C_4 competition model,
538 and the SPLASH model can be found at [DOI: 10.5281/zenodo.8366848](https://doi.org/10.5281/zenodo.8366848) (Orme and Marion,
539 2023). The codes used for model coupling and experiment analysis used in this paper is
540 available at DOI: 10.5281/zenodo.14257604.

541 Supplement.

542 Supplementary Information is available for this paper.

543 Author Contributions

544 JZ, SPH and ICP designed the study. BZ provided model code. JZ ran the experiments. JZ and
545 SPH conducted the analyses. SPH wrote the first version of the manuscript and all co-authors
546 contributed to the final version.

547 Competing Interests

548 None of the authors has any competing interests.

549 Financial Support and Acknowledgements

550 JZ and SPH acknowledge NERC funding for the project "When and Why does it Rain in the
551 Desert: Utilising unique stalagmite and dust records on the northern edge of the Sahara". This
552 work is a contribution to the LEMONTREE (Land Ecosystem Models based On New Theory,
553 obseRvations and ExperimEnts) project (SPH, ICP). LEMONTREE research received support
554 through Schmidt Sciences, LLC. ICP also acknowledges funding from the European Research
555 Council for the project REALM (Re-inventing Ecosystem And Land-surface Models, Grant
556 Number 787203).
557

References

Archer, S.R., Andersen, E.M., Predick, K.I., Schwinning, S., Steidl, R.J., and Woods, S.R.: Woody plant encroachment: Causes and consequences. In: Briske, D. (Ed.), Rangeland Systems. Springer Series on Environmental Management. Springer, Cham. https://doi.org/10.1007/978-3-319-46709-2_2, 2017.

Berger, A. L.: Long-term variations of caloric insolation resulting from the earth's orbital elements, *Quat. Res.*, 9, 139–167, 1978.

Berger, A., and Loutre, M. F.: insolation values for the climate of the last 10 000 000 years, *Quat. Sci. Rev.*, 10, 297–317, [https://doi.org/10.1016/0277-3791\(91\)90033-q](https://doi.org/10.1016/0277-3791(91)90033-q), 1991.

Bonan, G. B.: Forests and climate change: Forcings, feedbacks, and the climate benefits of forests, *Science*, 320, 1444–1449, 2008.

Bragg, F., Prentice, I.C., Harrison, S.P., Foster, P.N., Eglinton, G., Rommerskirchen F., and Rullkötter, J.: n-Alkane stable isotope evidence for CO₂ as a driver of vegetation change, *Biogeosci.*, 10, 2001–2010, 2013.

Brierley, C., Zhao, A., Harrison, S.P., Braconnot, P., Williams, C., Thornalley, D., Shi, X., Peterschmitt, J.-Y., Ohgaito, R., Kaufman, D.S., Kagayama, M., Hargreaves, J.C., Erb, M., Emile-Geay, J., D'Agostino, R., Chandan, D., Carré, M., Bartlein, P.J., Zheng, W., Zhang, Z., Zhang, Q., Yang, H., Volodin, E.M., Routsen, C., Peltier, W.R., Otto-Bliesner, B., Morozova, P.A., McKay, N.P., Lohmann, G., LeGrande, A.N., Guo, C., Cao, J., Brady, E., Annan, J.D., and Abe-Ouchi, A.: Large-scale features and evaluation of the PMIP4-CMIP6 *midHolocene* simulations, *Clim. Past*, 16, 1847–1872, 2020.

Cai, W., and Prentice, I.C.: Recent trends in gross primary production and their drivers: analysis and modelling at flux-site and global scales, *Environ. Res. Lett.*, 15, 124050, 2020.

Cai, W., Zhu, Z., Harrison, S.P., Ryu, Y., Wang, H., Zhou, B., and Prentice, I.C.: A unifying principle for global greenness patterns and trends, *Nat. Comm. Environ.*, 6, 19, <https://doi.org/10.1038/s43247-025-01992-0>, 2025.

Chen, J.M., Ju, W., Ciais, P., Viovy, N., Liu, R., Liu, Y., and Lu, X.: Vegetation structural change since 1981 significantly enhanced the terrestrial carbon sink, *Nat. Commun.*, 10, 4259, <https://doi.org/10.1038/s41467-019-12257-8>, 2019.

Chen, W., Zhu, D., Ciais, P., Huang, C., Viovy, N., and Kageyama, M.: Response of vegetation cover to CO₂ and climate changes between Last Glacial Maximum and pre-industrial period in a dynamic global vegetation model, *Quat. Sci. Rev.*, 218, 293–305, <https://doi.org/10.1016/j.quascirev.2019.06.003>, 2019.

Ciais, P., Tagliabue, A., Cuntz, M., Bopp, L., Scholze, M., Hoffmann, G., Laurantou, A., Harrison, S.P., Prentice, I.C., Kelley, D.I., Kovan, C. and Piao, S.L.: Large inert carbon pool in the terrestrial biosphere at the Last Glacial Maximum, *Nature Geosci.*, 5, 74–79, 10.1038/NGEO1324, 2011.

Claussen, M., Selent, K., Brovkin, V., Raddatz, T., and Gayler, V.: Impact of CO₂ and climate on Last Glacial maximum vegetation – a factor separation, *Biogeosci.*, 10, 3593–360, <https://bg.copernicus.org/articles/10/3593/2013/>, 2013.

Cotton, J.M., Cerling, T.E., Hoppe, K.A., Mosier, T.M., and Still, C.J.: Climate, CO₂, and the history of North American grasses since the Last Glacial Maximum, *Sci. Adv.*, 2, e1501346, doi:10.1126/sciadv.1501346, 2016.

Cowling, S.A., and Sykes, M.T.: Physiological significance of low atmospheric CO₂ for plant-climate interactions. *Quat. Res.* 52, 237–242, 1999.

Davis, T.W., Prentice, I.C., Stocker, B.D., Thomas, R.T., Whitley, R.J., Wang, H., Evans, B. J., Gallego-Sala, A.V., Sykes, M.T., and Cramer, W.: Simple process-led algorithms for simulating habitats (SPLASH v.1.0): robust indices of radiation,

Formatted: Left

Deleted: *BioRxiv*
doi: <https://doi.org/10.1101/2023.02.25.529932> (2023)

Deleted: in review

Deleted: 4

Formatted: Font: Ligatures: None

- evapotranspiration and plant-available moisture, *Geosci. Model Dev.*, 10, 689–708, <https://doi.org/10.5194/gmd-10-689-2017>, 2017.
- Diefendorf, A. F., Mueller, K. E., Wing, S. L., Koch, P. L., and Freeman, K. H.: Global patterns in leaf ^{13}C discrimination and implications for studies of past and future climate, *P. Natl. Acad. Sci. USA*, 107, 5738–5743, 2010.
- Eglinton, T. I. and Eglinton, G.: Molecular proxies for paleoclimatology. *Earth Planet. Sci. Lett.*, 275, 1–16, 2008.
- Farquhar, G.D., von Caemmerer, S., and Berry, J.A.: A biochemical model of photosynthetic CO_2 assimilation in leaves of C_3 species, *Planta*, 149, 78–90, 1980.
- Flores, O., Gritti, E.S., and Jolly, D.: Climate and CO_2 modulate the C_3/C_4 balance and $\delta^{13}\text{C}$ signal in simulated vegetation, *Clim. Past*, 5, 431–440, 2009.
- Foley, J.A.: [The sensitivity of the terrestrial biosphere to climatic change: A simulation of the Middle Holocene](#), *Glob. Biogeochem. Cycles*, 8, 505–525, doi:10.1029/94GB01636, 1994.
- Forzieri, G., Miralles, D. G., Ciais, P., Alkama, R., Ryu, Y., Duveiller, G., Zhang, K., Robertson, E., Kautz, M., Martens, B., Jiang, C., Arneth, A., Georgievski, G., Li, W., Ceccherini, G., Anthoni, P., Lawrence, P., Wiltshire, A., Pongratz, J., ... Cescatti, A.: Increased control of vegetation on global terrestrial energy fluxes, *Nature Clim. Change*, 10, 356–362. <https://doi.org/10.1038/s41558-020-0717-0>, 2020.
- François, L.M., Delire, C., Warnant, P., and Munhoven, G.: Modelling the glacial–interglacial changes in the continental biosphere, *Glob. Planet. Change*, 16–17, 37–52, [https://doi.org/10.1016/S0921-8181\(98\)00005-8](https://doi.org/10.1016/S0921-8181(98)00005-8), 1998.
- Francois, L., Godderis, Y., Warnant, P., Ramstein, G., de Noblet, N., and Lorenz, S.: [Carbon stocks and isotopic budgets of the terrestrial biosphere at mid-Holocene and last glacial maximum times](#), *Chem. Geol.*, 159, 163–189, 1999.
- Galy, V., François, L., France-Lanord, C., Faure, P., Kudrass, H., Palhol, F., and Singh, S.K.: C_4 plants decline in the Himalayan basin since the Last Glacial Maximum, *Quat. Sci. Rev.*, 27, 1396–1409, <https://doi.org/10.1016/j.quascirev.2008.04.005>, 2008.
- Gerhart, L.M., and Ward, J.K.: Plant responses to low $[\text{CO}_2]$ of the past, *New Phytol.*, 188, 674–695, <https://doi.org/10.1111/j.1469-8137.2010.03441.x>, 2010.
- Haas, O., Prentice, I.C., and Harrison, S.P.: [Examining the response of wildfire properties to climate and atmospheric \$\text{CO}_2\$ change at the Last Glacial Maximum](#), *Biogeosci.*, 20, 3981–3995, <https://doi.org/10.5194/bg-20-3981-2023>, 2023.
- Harrison, S.P., and Prentice, I.C.: Climate and CO_2 controls on global vegetation distribution at the last Glacial Maximum: analysis based on palaeovegetation data, biome modelling and palaeoclimate simulations, *Glob. Chang. Biol.*, 9, 983–1004, 2003
- Harrison, S.P., Cramer, W., Franklin, O., Prentice, I.C., Wang, H., Brännström, Å., de Boer, H., Dieckmann, U., Joshi, J., Keenan, T.F., Lavergne, A., Manzoni, S., Mengoli, G., Morfopoulos, C., Peñuelas, J., Pietsch, S., Rebel, K.T., Ryu, Y., Smith, N.G., Stocker, B.D., and Wright, I.J.: [Eco-evolutionary optimality as a means to improve vegetation and land-surface models](#), *New Phytol.*, 231, 2125–2141, <https://doi.org/10.1111/nph.17558>, 2021.
- Haverd, V., Smith, B., Canadell, J.G., Cuntz, M., Mikaloff-Fletcher, S., Farquhar, G., Woodgate, W., Briggs, P.R., and Trudinger, C.M.: Higher than expected CO_2 fertilization inferred from leaf to global observations, *Glob. Chang. Biol.* 26, 2390–2402, <https://doi.org/10.1111/gcb.14950>, 2020.
- Hoek van Dijke, A. J., Mallick, K., Schlerf, M., Machwitz, M., Herold, M., and Teuling, A. J.: Examining the link between vegetation leaf area and land–atmosphere exchange of water, energy, and carbon fluxes using FLUXNET data, *Biogeosci.*, 17, 4443–4457, <https://doi.org/10.5194/bg-17-4443-2020>, 2020.

661 Hoogakker, B.A.A., Smith, R.S., Singarayer, J.S., Marchant, R., Prentice, I.C., Allen, J.R.M.,
662 Anderson, R.S., Bhagwat, S.A., Behling, H., Borisova, O., Bush, M., Correa-Metrio,
663 A., de Vernal, A., Finch, J.M., Fréchette, B., Lozano-Garcia, S., Gosling, W.D.,
664 Granoszewski, W., Grimm, E.C., Grüger, E., Hanselman, J., Harrison, S.P., Hill, T.R.,
665 Huntley, B., Jiménez-Moreno, G., Kershaw, P., Ledru, M-P., Magri, D., McKenzie, M.,
666 Müller, U., Nakagawa, T., Novenko, E., Penny, D., Sadori, L., Scott, L., Stevenson, J.,
667 Valdes, P.J., Vandergoes, M., Velichko, A., Whitlock, C., and Tzedakis, C.: Terrestrial
668 biosphere changes over the last 120 kyr, *Clim. Past*, 12, 51–73,
669 <https://doi.org/10.5194/cp-12-51-2016>, 2016.

670 Izumi, K., Bartlein, P.J., and Harrison, S.P.: Consistent behaviour of the climate system in
671 response to past and future forcing, *Geophys. Res. Lett.*, 40, 1817–1823,
672 doi:10.1002/grl.50350, 2013.

673 Jiang, C., Ryu, Y., Wang, H., and Keenan, T.F.: An optimality-based model explains seasonal
674 variation in C₃ plant photosynthetic capacity, *Glob. Change Biol.*, 26, 6493–6510,
675 2020.

676 Jiang, W., Wu, H., Li, Q., Lin, Y., and Yu, Y.: Spatiotemporal changes in C₄ plant abundance
677 in China since the Last Glacial Maximum and their driving factors, *Palaeogeog.*,
678 *Palaeoclim.*, *Palaeoecol.*, 518, 10–21, <https://doi.org/10.1016/j.palaeo.2018.12.021>,
679 2019.

680 Jolly, D., and Haxeltine, A.: Effect of low glacial atmospheric CO₂ on tropical African
681 montane vegetation, *Science*, 276, 786–788, 1997.

682 Kageyama, M., Albani, S., Braconnot, P., Harrison, S.P., Hopcroft, P.O., Ivanovic, R.F.,
683 Lambert, F., Marti, O., Peltier, W.R., Peterschmidt, J.-Y., Roche, D.M., Tarasov, L.,
684 Zhang, X., Brady, E., Haywood, A.M., LeGrande, A., Lunt, D.J., Mahowald, N.M.,
685 Mikolajewicz, U., Nisancioglu, K.H., Otto-Bliesner, B.L., Renssen, H., Tomas, B.,
686 Zhang, Q., Abe-Ouchi, A., Bartlein, P.J., Cao, J., Lohmann, G., Ohgaito, R., Shi, X.,
687 Volodin, E., Yoshida, K., Zhang, X., and Zheng, W.: The PMIP4 contribution to
688 CMIP6 – Part 4: Scientific objectives and experimental design of the PMIP4-CMIP6
689 Last Glacial Maximum experiments and PMIP4 sensitivity experiments, *Geosci.*
690 *Model Dev.*, 10, 4035–4055, <https://doi.org/10.5194/gmd-10-4035-2017>, 2017

691 Kageyama, M., Harrison, S.P., Kapsch, M., Lofverstrom, M., Lora, J.M., Mikolajewicz, U.,
692 Sherriff-Tadano, S., Vadsaria, T., Abe-Ouchi, A., Bouttes, N., Chandan, D., LeGrande,
693 A.N., Lhardy, F., Lohmann, G., Morozova, P.A., Ohgaito, R., Peltier, W.R., Quiquet,
694 A., Roche, D.M., Shi, X., Schmittner, A., Tierney, J.E., and Volodin, E.: The PMIP4-
695 CMIP6 Last Glacial Maximum experiments: preliminary results and comparison with
696 the PMIP3-CMIP5 simulations, *Clim. Past*, 17, 1065–1089, 2021.

697 Kaplan, J.O., Bigelow, N.H., Bartlein, P.J., Christensen, T.R., Cramer, W., Harrison, S.P.,
698 Matveyeva, N.V., McGuire, A.D., Murray, D.F., Prentice, I.C., Razzhivin, V.Y., Smith,
699 B. and Walker, D.A., Anderson, P.M., Andreev, A.A., Brubaker, L.B., Edwards, M.E.,
700 and Lozhkin, A.V.: Climate change and Arctic ecosystems II: Modeling, palaeodata-
701 model comparisons, and future projections, *J. Geophys. Res.- Atmos.*, 108, 8171. doi:
702 10.1029/2002JD002559, 2003.

703 Kattge, J., Diaz, S., Lavorel, S., Prentice, I.C., Leadley, P., Bönisch, G., Garnier, E., Westoby,
704 M., Reich, P.B., Wright, I.J., Cornelissen, J.H.C., Violle, C., Harrison, S.P., van
705 Bodegom, P.M., Reichstein, M., Soudzilovskaia, N.A., Ackerly, D.D., Anand, M.,
706 Atkin, O., Bahn, M., Baker, T.R., Baldocchi, D., Bekker, R., Blanco, C., Blonder, B.,
707 Bond, W., Bradstock, R., Bunker, D.E., Casanoves, F., Cavender-Bares, J., Chambers,
708 J., Chapin, F.S., Chave, J., Coomes, D., Cornwell, W.K., Craine, J.M., Dobrin, B.H.,
709 Durka, W., Elser, J., Enquist, B.J., Esser, G., Estiarte, M., Fagan, W.F., Fang, J.,
710 Fernández, F., Fidelis, A., Finegan, B., Flores, O., Ford, H., Frank, D., Freschet, G.T.,

Moved down [1]: Kaplan, J.O., Bigelow, N.H., Bartlein, P.J., Christensen, T.R., Cramer, W., Harrison, S.P., Matveyeva, N.V., McGuire, A.D., Murray, D.F., Prentice, I.C., Razzhivin, V.Y., Smith, B. and Walker, D.A., Anderson, P.M., Andreev, A.A., Brubaker, L.B., Edwards, M.E., and Lozhkin, A.V.: Climate change and Arctic ecosystems II: Modeling, palaeodata-model comparisons, and future projections, *J. Geophys. Res.- Atmos.*, 108, 8171. doi: 10.1029/2002JD002559, 2003.

Deleted: ¶

Moved (insertion) [1]

- Fyllas, N.M., Gallagher, R., Green, W., Gutierrez, A.G., Hickler, T., Higgins, S., Hodgson, J.G., Jalili, A., Jansen, S., Kerkhoff, A.J., Kirkup, D., Kitajima, K., Kleyer, M., Klotz, S., Knops, J.M.H., Kramer, K., Kühn, I., Kurokawa, H., Laughlin, D., Lee, T.D., Leishman, M., Lens, F., Lenz, T., Lewis, S.L., Lloyd, J., Llusà, J., Louault, F., Ma, S., Mahecha, M.D., Manning, P., Massad, T., Medlyn, B., Messier, J., Moles, A., Müller, S., Nadrowski, K., Naeem, S., Niinemets, U., Nöllert, S., Nüske, A., Ogaya, R., Joleksyn, J., Onipchenko, V.G., Onoda, Y., Ordoñez, J., Overbeck, G., Ozinga, W., Patiño, S., Paula, S., Pausas, J.G., Peñuelas, J., Phillips, O.L., Pillar, V., Poorter, H., Poorter, L., Poschlod, P., Proulx, R., Rammig, A., Reinsch, S., Reu, B., Sack, L., Salgado, B., Sardans, J., Shiodera, S., Shipley, B., Sosinski, E., Soussana, J-F., Swaine, E., Swenson, N., Thompson, K., Thornton, P., Waldram, M., Weiher, E., White, M., Wright, S.J., Zaehle, S., Zanne, A.E., and Wirth, C.: TRY – a global database of plant traits, *Glob. Change Biol.*, 17, 2905–2935, doi:10.1111/j.1365-2486.2011.02451.x, 2011.
- Keenan, T.F., Hollinger, D.Y., Bohrer, G., Dragoni, D., Munger, J.W., Schmid, H.P., and Richardson, A.D.: Increase in forest water-use efficiency as atmospheric carbon dioxide concentrations rise, *Nature*, 499, 324–327, 2013.
- Landaïs, A., Lathiere, J., Barkan, E., and Luz, B.: Reconsidering the change in global biosphere productivity between the Last Glacial Maximum and present day from the triple oxygen isotopic composition of air trapped in ice cores, *Glob. Biogeochem. Cyc.*, 21, GB1025, 2007.
- Lavergne, A., Harrison, S.P., Atsawawaranunt, K., Dong, N., and Prentice, I.C.: Recent C4 vegetation decline is imprinted in land carbon isotopes. *Nature Comm. Earth Environ.*, in review, 2024
- Lavergne, A., Voelker, S., Csank, A., Graven, H., de Boer, H.J., Daux, V., Robertson, I., Dorado-Liñan, I., Martinez-Sancho, E., Battipaglia, G. et al.: Historical changes in the stomatal limitation of photosynthesis: empirical support for an optimality principle, *New Phytol.*, 225, 2484–2497, 2020.
- Levis, S., Foley, J.A., and Pollard, D.: CO₂, climate, and vegetation feedbacks at the Last Glacial Maximum, *J. Geophys. Res.*, 104, 31191–31198, 1999.
- Li, G., Harrison, S. P., Bartlein, P. J., Izumi, K., and Prentice, I. C.: Precipitation scaling with temperature in warm and cold climates: an analysis of CMIP5 simulations, *Geophys. Res. Lett.*, 40, 4018– 4024, <https://doi.org/10.1002/grl.50730>, 2013.
- Makou, M.C., Hughen, K.A., Xu, L., Sylva, S.P., and Eglinton, T.I.: Isotopic records of tropical vegetation and climate change from terrestrial vascular plant biomarkers preserved in Cariaco Basin sediments, *Org. Geochem.*, 38, 1680-1691, <https://doi.org/10.1016/j.orggeochem.2007.06.003>, 2007.
- Marchant, R.A., Harrison, S.P., Hooghiemstra, H., Markgraf, V., Boxel, J.H., Ager, T., Almeida, L., Anderson, R., Baied, C., Behling, H., Berrio, J.C., Burbridge, R., Björck, S., Byrne, R., Bush, M.B., Cleef, A.M., Duivenvoorden, J.F., Flenley, J.R., de Oliveira, P.E., van Geel, B., Graf, K.J., Gosling, W.D., Harbele, S., van der Hammen, T., Hansen, B.C.S., Horn, S.P., Islebe, G.A., Kuhry, P., Ledru, M-P., Mayle, F.E., Leyden, B.W., Lozano-Garcia, M.S., Lozano-Garcia, S., Melief, A.B.M., Moreno, P., Moar, N.T., Prieto, A., van Reenan, G.B., Salgado-Labouriau, M.L., Schäbitz, F., Schreve-Brinkman, E.J., and Wille, M.: Pollen-based biome reconstructions for Latin America at 0, 6000 and 18 000 radiocarbon years, *Clim. Past*, 5, 725-767, 2009
- Martin Calvo, M., and Prentice, I.C.: Effects of fire and CO₂ on biogeography and primary production in glacial and modern climates, *New Phytol.*, 208, 987-994, 2015.

- [Martin Calvo, M., Prentice, I.C., and Harrison, S.P.: Climate versus carbon dioxide controls on biomass burning: a model analysis of the glacial-interglacial contrast, *Biogeosci.*, 11, 6017–6027, 2014.](#)
- Mauritsen, T., Bader, J., Becker, T., Behrens, J., Bittner, M., Brokopf, R., et al.: Developments in the MPI-M Earth System Model version 1.2 (MPI-ESM1.2) and its response to increasing CO₂, *J. Advan. Modeling Earth Systems*, 11, 998–1038, <https://doi.org/10.1029/2018MS001400>, 2019.
- Medlyn, B.E., De Kauwe, M.G., Lin, Y.-S., Knauer, J., Duursma, R.A., Williams, C.A., Arneeth, A., Clement, R., Isaac, P., Limousin, J.-M., Linderson, M.-L., Meir, P., Martin-StPaul, N., and Wingate, L.: How do leaf and ecosystem measures of water-use efficiency compare?, *New Phytol.*, 216, 758–770, <https://doi.org/10.1111/nph.14626>, 2017.
- [O'ishi, R., and Abe-Ouchi, A.: Influence of dynamic vegetation on climate change and terrestrial carbon storage in the Last Glacial Maximum, *Clim. Past*, 9, 1571–1587, <https://doi.org/10.5194/cp-9-1571-2013>, 2013.](#)
- Otto-Bliesner, B.L., Braconnot, P., Harrison, S.P., Lunt, D.J., Abe-Ouchi, A., Albani, S., Bartlein, P.J., Capron, E., Carlson, A.E., Dutton, A., Fischer, H., Goelzer, H., Govin, A., Haywood, A., Joos, F., Legrande, A.N., Lipscomb, W.H., Lohmann, G., Mahowald, N., Nehrbass-Ahles, C., Pausata, F.S.R., Peterschmidt, J.-Y., Phipps, S.J., Renssen, R., and Zhang, Q.: The PMIP4 contribution to CMIP6 – Part 2: Two interglacials, scientific objective and experimental design for Holocene and Last Interglacial simulations, *Geosci. Model Dev.*, 10, 3979–4003, <https://doi.org/10.5194/gmd-10-1-2017>, 2017.
- Piao, S., Friedlingstein, P., Ciais, P., Zhou, L., and Chen, A.: Effect of climate and CO₂ changes on the greening of the Northern Hemisphere over the past two decades. *Geophys. Res. Lett.* 33, L23402, <https://doi.org/10.1029/2006GL028205>, 2006.
- Piao, S., Wang, X., Park, T., Chen, C., Lian, X., He, Y., Bjerke, J. W., Chen, A., Ciais, P., Tømmervik, H., Nemani, R. R., and Myneni, R. B.: Characteristics, drivers and feedbacks of global greening, *Nature Rev. Earth Environ.*, 1, 14–27. <https://doi.org/10.1038/s43017-019-0001-x>, 2020.
- Peng, Y., Bloomfield, K.J., and Prentice, I.C.: A theory of plant function helps to explain leaf-trait and productivity responses to elevation, *New Phytol.*, 226, 1274–1284, 2020.
- Pickett, E.J., Harrison, S.P., Hope, G., Harle, K., Dodson, J.R., Kershaw, A.P., Prentice, I.C., Backhouse, J., Colhoun, E.A., D'Costa, D., Flenley, J., Grindrod, J., Haberle, S., Hassell, C., Kenyon, C., Macphail, M., Martin, H., Martin, A.H., McKenzie, M., Newsome, J.C., Penny, D., Powell, J., Raine, J.I., Southern, W., Stevenson, J., Sutra, J.P., Thomas, I., van der Kaars, S., and Ward, J.: Pollen-based reconstructions of biome distributions for Australia, Southeast Asia and the Pacific (SEAPAC region) at 0, 6000 and 18,000 ¹⁴C yr B.P. *Journal of Biogeography* 31: 1381–1444, [10.1111/j.1365-2699.2004.01001.x](https://doi.org/10.1111/j.1365-2699.2004.01001.x), 2004.
- Polley, H.W., Johnson, H.B., Marino, B.D., and Mayeux, H.S.: Increases in C₃ plant water-use efficiency and biomass over glacial to present CO₂ concentrations, *Nature*, 361, 61–64, 1993.
- Prentice, I.C., Dong, N., Gleason, S.M., Maire, V., Wright, I.J.: Balancing the costs of carbon gain and water transport: testing a new theoretical framework for plant functional ecology, *Ecol. Lett.*, 17, 82–91, 2014.
- Prentice, I.C., Harrison, S.P., and Bartlein P.J.: Global vegetation and terrestrial carbon cycle changes after the last ice age, *New Phytol.*, 189, 988–998, 2011.

815 Prentice, I.C., Jolly, D., and BIOME 6000 Participants, 2000. Mid-Holocene and glacial-
816 maximum vegetation geography of the northern continents and Africa, *J. Biogeog.*, 27:
817 507-519.

818 Prentice, I.C., Kelley, D.I., Foster, P.N., Friedlingstein, P., Harrison, S.P., and Bartlein, P.J.:
819 Modeling fire and the terrestrial carbon balance, *Glob. Biogeochem. Cycl.*, 25,
820 GB3005, doi:10.1029/2010GB003906, 2011.

821 Rommelskirchen, F., Eglinton, G., Dupont, L., and Rullkötter, J.: Glacial/interglacial changes
822 in southern Africa: Compound-specific $\delta^{13}\text{C}$ land plant biomarker and pollen records
823 from southeast Atlantic continental margin sediments, *Geochem. Geophys. Geosy.*, 7,
824 Q08010, 2006.

825 Sato, H., Kelley, D.I., Mayor, S.J., Martin Calvo, M., Cowling, S.A., and Prentice, I.C.: Dry
826 corridors opened by fire and low CO_2 in Amazonian rainforest during the Last Glacial
827 Maximum, *Nat. Geosci.*, 14, 578–585, <https://doi.org/10.1038/s41561-021-00777-2>,
828 2021.

829 Sinninghe Damsté, J. S., Verschuren, D., Ossebaer, J., Blokker, J., van Houten, R., Plessen,
830 B., and Schouten, S.: A 25,000-year record of climate-induced changes in lowland
831 vegetation of eastern equatorial Africa revealed by the stable carbon-isotopic
832 composition of fossil plant leaf waxes, *Earth Planet. Sci. Lett.*, 302, 236–246, 2011.

833 Smith, N.G., and Keenan, T.F.: Mechanisms underlying leaf photosynthetic acclimation to
834 warming and elevated CO_2 as inferred from least-cost optimality theory, *Glob.*
835 *Change Biol.*, 26, 5202–5216, 2020.

836 Smith, N.G., Keenan, T.F., Prentice, I.C., Wang, H., Wright, I.J., Niinemets, U., Crous, Y.,
837 Domingues, T.F., Guerrieri, R., Ishida, F.Y., Kattge, J., Kruger, E.L., Maire, V.,
838 Rogers, A., Serbin, S.P., Tarvainen, L., Togashi, H.F., Townsend, P.A., Wang, M.,
839 Weerasinghe, L.K., and Zhou, S.-X.: Global photosynthetic capacity is optimized to
840 the environment, *Ecol. Lett.*, 22, 506–517, 2019.

841 Stein, U., and Alpert, P.: Factor separation in numerical simulations, *J. Atmos. Sci.*, 50, 2107–
842 2115, 1993.

843 Stocker, B.D., Wang, H., Smith, N.G., Harrison, S.P., Keenan, T., Sandoval, D., Davis, T., and
844 Prentice, I.C.: P-model v1.0: an optimality-based light use efficiency model for
845 terrestrial gross primary production, *Geosci. Model Devel.*, 13, 1545–1581, 2020.

846 Swinehart, D.F.: The Beer-Lambert Law, *J. Chem. Educ.*, 39, 333,
847 <https://doi.org/10.1021/ed039p333>, 1962.

848 Vogts, A., Schefuß, E., Badewien, T., and Rullkötter, J.: n-alkane parameters derived from a
849 deep-sea sediment transect off south-west Africa reflect continental vegetation and
850 climate conditions, *Org. Geochem.*, 47, 109–119, 2012.

851 [Wang, H., Atkin, O.K., Keenan, T.F., Smith, N.G., Wright, I.J., Bloomfield, K.J., Kattge, J.,](#)
852 [Reich, P.B., and Prentice, I.C.: Acclimation of leaf respiration consistent with optimal](#)
853 [photosynthetic capacity, *Glob. Change Biol.*, 26, 2573–2583, 2020.](#)

854 Wang, H., Prentice, I.C., Cornwell, W.M., Keenan, T.F., Davis, T.W., Wright, I.J., Evans, B.J.,
855 and Peng, C.: Towards a universal model for carbon dioxide uptake by plants. *Nature*
856 *Plants*, 3, 734–741, 2017.

857 Williams, I.N., and Torn, M.S.: Vegetation controls on surface heat flux partitioning, and
858 land-atmosphere coupling, *Geophys. Res. Lett.*, 42, 9416–9424,
859 doi:10.1002/2015GL066305, 2015.

860 Williams, J.W.: Variations in tree cover in North America since the last glacial maximum, *Glob.*
861 *Planet. Change*, 35, 1-23, [https://doi.org/10.1016/S0921-8181\(02\)00088-7](https://doi.org/10.1016/S0921-8181(02)00088-7), 2003.

862 Wohlfahrt, J., Harrison, S.P., Braconnot, P., Hewitt, C.D., Kutzbach, J.E., Kitoh, A.,
863 Mikolajewicz, U., Otto-Bliesner, B., and Weber, N.: Evaluation of coupled ocean-

atmosphere simulations of northern hemisphere extratropical climates in the mid-Holocene, *Clim. Dyn.*, 31, 871–890, 10.1007/s00382-008-0415-5, 2008.

Willez, M.-N., Kageyama, M., Krinner, G., de Noblet-Ducoudré, N., Viovy, N., and Mancip, M.: Impact of CO₂ and climate on the Last Glacial Maximum vegetation: results from the ORCHIDEE/IPSL models, *Clim. Past*, 7, 557–577, <https://doi.org/10.5194/cp-7-557-2011>, 2011.

Xu, H., Wang, H., Prentice, I.C., Harrison, S.P., Wang, G., and Sun, X.: Predictability of leaf traits with climate and elevation: a case study in Gongga Mountain, China, *Tree Physiol.*, doi: 10.1093/treephys/tpab003, 2021.

Yang, J.-W., Brandon, M., Landais, A., Duchamp-Alphonse, S., Blunier, T., Prie, F., and Extier, T.: Global biosphere primary productivity changes during the past eight glacial cycles, *Science*, 375, 1145–115, 10.1126/science.abj8826, 2022.

Zeng, Z., Piao, S., Li, L., Zhou, L., Ciais, P., Wang, T., Li, Y., Lian, X., Wood, E. F., Friedlingstein, P., Mao, J., Estes, L.D., Myneni, R.B., Peng, S., Shi, X., Seneviratne, S.I., and Wang, Y.: Climate mitigation from vegetation biophysical feedbacks during the past three decades, *Nature Clim. Change*, 7, 432–436, <https://doi.org/10.1038/nclimate3299>, 2017.

Zhou, B., Cai, W., Zhu, Z., Wang, H., Harrison, S.P., and Prentice, I.C.: A general model for the seasonal to decadal dynamics of leaf area, *Glob. Change Biol.*, e70125, <https://doi.org/10.1111/gcb.70125>, 2025.

Zhu, Z., Wang, H., Harrison, S.P., Prentice, I.C., Qiao, S., and Tan, S.: Optimality principles explaining divergent responses of alpine vegetation to environmental change, *Glob. Change Biol.*, 29, 126–142, doi: 10.1111/gcb.16459, 2022.

Deleted:

Deleted: bioRxiv, <https://www.biorxiv.org/content/10.1101/2024.10.23.619947v1>, 2024

Deleted: .